Optical Spectroscopic Characterization of Single Tryptophan Mutants of Chicken Skeletal Troponin C: Evidence for Interdomain Interaction†

Martin C. Moncrieffe,*,‡ Sergei Yu. Venyaminov,‡ Todd E. Miller,§ Georgiana Guzman,§ James D. Potter,§ and Franklyn G. Prendergast*,‡

Department of Biochemistry and Molecular Biology, Mayo Foundation, 200 First Street SW, Rochester, Minnesota 55905, and Department of Molecular and Cellular Pharmacology, University of Miami School of Medicine, Miami, Florida 33101

Received August 24, 1998; Revised Manuscript Received June 30, 1999

ABSTRACT: The effects of metal ion binding on the optical spectroscopic properties and temperature stability of two single tryptophan mutants of chicken skeletal TnC, F78W and F154W, have been examined. The absence of tyrosine and other tryptophan residues allowed the unambiguous assignment of the spectral signal from the introduced Trp residue. Changes in the molar ellipticity values in the far-UV CD spectra of the mutant proteins on metal ion binding were similar to those of wild-type TnC suggesting that the introduction of the Trp residue had no effect on the total secondary structure content. The fluorescence and near-UV absorbance data reveal that, in the apo state, Trp-78 is buried while Trp-154 is exposed to solvent. Additionally, the highly resolved ^1L_b band of Trp-78 seen in the near-UV absorbance and CD spectra of the apo state of F78W suggest that this residue is likely in a rigid molecular environment. In the calcium-saturated state, Trp-154 becomes buried while the solvent accessibility of Trp-78 increases. The fluorescence emission and near-UV CD of Trp-78 in the N-terminal domain were sensitive to calcium binding at the C-terminal domain sites. Measurements of the temperature stability reveal that events occurring in the N-terminal domain affect the stability of the C-terminal domain and vice versa. This, coupled with the titration data, strongly suggests that there are interactions between the N- and C-terminal domains of TnC.

Troponin C (TnC),[1] the calcium-binding component of the troponin complex, plays a crucial role in the calcium-induced regulation of skeletal muscle contraction and relaxation. The crystal structure of TnC (*1*, *2*) revealed a dumbbell-shaped molecule of length 75 Å whose N- and C-terminal lobes are approximately 25 Å in diameter and are separated by an extended α-helix. Each lobe contains two metal ion binding sites arranged in a helix−loop−helix EF-hand motif (*3*) in which the calcium ion is six-coordinated to a 12 residue loop. The sites in the N-terminal half of the molecule (I and II) are referred to as the calcium specific sites ($K_{a,Ca} \approx 10^5$ M^{-1}) while those in the C-terminal domain (III and IV) bind both calcium and magnesium ($K_{a,Mg} \approx 10^3$ M^{-1} and $K_{a,Ca} \approx 10^7$ M^{-1}) (*4*). A structural role has been ascribed to the C-terminal sites (*5*), and this assignment is supported by the observation that mutants of TnC in which sites III and IV have been inactivated are capable of restoring calcium-dependent muscle contraction to TnC-depleted skinned fibers. Such mutants however, were easily removed by washing the fibers (*6*−*8*). In contrast, the inactivation of sites I and II resulted in mutants that were incapable of restoring muscle contraction in a calcium-dependent manner suggesting that these sites functioned in a regulatory capacity. Additionally, the rate of dissociation of calcium ions from sites I and II is much greater than that from III and IV, as would be expected of regulatory sites (*9*).

An intriguing issue related to the regulation of muscle contraction concerns the structural changes evoked by calcium binding to the calcium specific sites of TnC and how that signal is transmitted to the other members of the troponin complex. On the basis of the crystal structure of TnC bearing calcium at sites III and IV, Herzberg et al. (*10*) proposed a model (the HMJ model) of the calcium-induced conformational changes occurring in the regulatory N-terminal domain. This model suggests that in the transition from the apo to the calcium-saturated state, the predominant structural change involves movement of the B/C helices away from the N/A/D helices, resulting in the exposure of a hydrophobic surface; the latter was proposed as the binding site for other members of the troponin complex, most notably troponin I (TnI) but possibly troponin T (TnT). The notion of such a hydrophobic patch in TnC is strongly supported by a wealth of experimental data (*11*−*17*) and conceptually by analogy to what has been found with calmodulin (*18*, *19*). More direct support comes from the recent NMR solution structure of calcium-saturated skeletal muscle TnC

† This work was supported by NIH Grants GM34847 to F.G.P. and AR37701 to J.D.P.

* Authors to whom correspondence should be addressed.

‡ Mayo Foundation.

§ University of Miami School of Medicine.

[1] Abbreviations: TnC, troponin C; CD, circular dichroism; Trp, tryptophan; Phe, phenylalanine; MOPS, 3-morpholinopropane sulfonic acid; EDTA, ethylenediaminetetraacetic acid; EGTA, ethylenebis-(oxyethylenenitrilo)tetraacetic acid; IPTG, isopropyl-D-thiogalactopyranoside; PMSF, (phenylmethyl)sulfonyl fluoride; TRIS, tris(hydroxymethyl)aminomethane hydrochloride; DTT, 1,4-dithiothreitol; $\Delta_{1/2}$, full-width at half-maximal amplitude; pCa, $-\log_{10}$ [free Ca^{2+}].

10.1021/bi982048j CCC: $18.00
Published on Web 08/26/1999

(*20*) and from the X-ray crystal structures of calcium-saturated TnC (*21*) and the calcium-saturated N-terminal domain of TnC (*22*).

However, a role for the C-terminal domain sites in the calcium-induced regulation of muscle contraction is not specifically addressed by the HMJ model (*10*). There is some evidence suggesting that interactions between the N- and C-terminal domains of TnC (*23*−*26*) and calmodulin (*27*, *28*) occur, but such interactions have not been definitively established (*29*, *30*). The finding that fragments of TnC-containing sites I and II were unable to fully restore force to extracted muscle fibers argues for a role of the C-terminal sites in calcium regulation and led François et al. (*31*) to speculate that interdomain interactions may be relevant to TnC function.

Whether the N- and C-terminal domains "communicate" with each other is clearly not an idle issue. While calcium binding to sites I and II in the N-terminal domain clearly provides the regulatory switch for muscle contraction as originally proposed by Potter and Gergely (*4*), the structural stability of the whole troponin complex must be sustained, at least in part, by the structure and stability of the magnesium and/or calcium replete C-terminal domain. Given the affinity constants of this domain for calcium (*4*) and that the minimum concentration of free calcium in the myoplasm, i.e., resting muscle is $\approx 10^{-7}$ M, it is likely that the C-terminal domain effectively anchors TnC helping it to sustain the interactions with TnI and TnT under conditions in which the N-terminal domain is calcium free and hence where the putative hydrophobic patch is not optimally "exposed".

This paper presents detailed characterization of the optical spectroscopic properties and temperature stability of two single tryptophan (Trp) mutants of chicken skeletal TnC. Such characterization is necessary if the observed spectral properties are to be interpreted in terms of a physical model of the conformational events that occur in TnC when it binds metal ions. This approach of using genetically inserted Trp residues to monitor conformational events in TnC has been used by several groups (*32*−*35*). The mutants used in this work are designated F78W and F154W have Phe → Trp substitutions at position $-z + 1$ of the EF-hand which is immediately after the last metal-ion-coordinating residue. Given the proximity of the introduced Trp residue to the metal binding sites, its spectroscopic properties should be influenced by ligand binding. Indeed, the optical spectral properties of F154W have been previously shown to be influenced by metal ion binding at the COOH-terminal domain sites of TnC (*36*). However, in the latter work, the details regarding the observed spectral changes were not discussed. Both F78W and F154W were isofunctional with wild-type TnC in the restoration of contractile activity to TnC-depleted muscle fibers (Potter et al., unpublished data).

Our results confirm previous reports (*29*, *37*) suggesting that direct metal ion binding to either the intact or separated domains of TnC confers increased stability to that domain. We have also found that events occurring in the N-terminal domain affect the stability of the C-terminal domain and vice versa. Additionally, Trp-78, located just after site II in the N-terminal in addition to being sensitive to calcium binding to the N-terminal domain sites (I and II), responds to calcium binding at the C-terminal domain sites. The ability of the N-terminal domain to respond to events in the C-terminal domain may be an important step in the mechanism by which the regulatory function of TnC is affected.

MATERIALS AND METHODS

Protein Preparation. A Trp codon (TGG) was introduced into the cDNA of wild-type chicken TnC by thermal cycling with mutagenic oligonucleotides to replace Phe (TTC) at positions 78 and 154. The sequences were confirmed using the Sequenase protocol (United States Biochemical). Proteins were expressed in *Escherichia coli* BL-21 cells and purified according to Szczesna (*8*). Briefly, DNA inserts were cloned into the Nco I−Bam-HI cloning site of the pET 3d plasmid vector (Novagen). Klenow enzyme was used to "blunt" cut the Bam-HI site so that ligation could be made with the "blunted" Hind-III site of the TnC DNA insert. After ligation and selection of plasmids containing the insert by restriction digestion, 100 ng of purified plasmid DNA was used to transform competent BL-21 cells according to Miller (*38*). Colonies were screened for overexpression of TnC as demonstrated on SDS PAGE gels. A single clone was selected and grown overnight in LB (DIFCO) with 100 μg/mL ampicillin, and 1 mL of a log phase subculture was inoculated into 2 L of enriched medium. After 12 h protein expression was induced with 0.4 mM IPTG, and cells were harvested 4 h later by centrifugation. The cell pellets were resuspended in 50 mM TRIS, pH 7.5, 1 M NaCl, 0.1 M $CaCl_2$, and 1 mM DTT with 1 μM leupeptin and pepstatin and 10 μM PMSF. The cell suspension was then sonicated, and the sonicates were cleared of bacterial debris by centrifugation, adjusted to 1 M ammonium sulfate, and recentrifuged. This supernatant was then applied to a 2.5 cm × 20 cm Phenyl Sepharose column equilibrated in cell resuspension buffer with 1 M ammonium sulfate to enhance the binding affinity of TnC. To minimize loss of loosely bound TnC, the column was washed with small amounts of the above solution and then eluted with a solution containing 50 mM TRIS, 2 mM EDTA, and 1 mM DTT (pH 7.5). TnC-containing fractions identified by SDS PAGE were dialyzed against a solution of 50 mM TRIS, 1 mM $CaCl_2$, 6 M urea, at pH 8.0, to equilibrium and applied to a 5 cm × 8 cm DE-52 column. The column was washed to remove all unbound protein before elution with a salt gradient of 0−500 mM KCl (2 × 300 mL). Fractions of greater than 95% purity were pooled and dialyzed against 5 mM ammonium bicarbonate, lyophilized, and stored at −70 °C before use.

Protein samples for spectral measurements were prepared by dissolving 2−3 mg of lyophilized protein in 1 mL of a medium composed of 120 mM MOPS, 90 mM KCl, and 2 mM EGTA at pH 7.0, and the resulting protein solution was dialyzed twice against 500 mL of a solution having the same composition. After dialysis, the volume was adjusted with dialysate to yield a protein concentration of approximately 1.5 mg/mL and this latter solution was diluted as required for the experiments detailed below. The high concentration of MOPS used ensured that the pH changes that accompany metal ion binding to TnC were negligible.

Fluorescence Spectroscopy. Fluorescence data were obtained at 20 °C using a MPF-66 (Perkin-Elmer), a Spex Fluorolog (Spex), or a FS900CDT (Edinburgh Instruments) spectrofluorometer. Protein concentrations were typically 7−10 μM for all fluorescence measurements. The excitation

wavelength was 280 nm, and the excitation and emission bandpass were 1 and 2 nm, respectively. Calcium titrations were conducted by adding aliquots of a $CaCl_2$ standard (Orion) to a calcium-free solution of the mutants and the emission spectrum after each addition was measured. The free calcium ion concentrations in these titrations was determined as described in Robertson and Potter (*39*) and covered the range pCa 9.5−3.5. Estimates of the apparent calcium association constants (K_i) for the TnC mutants were obtained by fitting the normalized integrated fluorescence intensity (over the range 300−420 nm), *f*, as a function of the free calcium ion concentration to eq 1 (*40*, *41*) where f_i

$$f = \sum_{i=1}^{2} f_i \frac{[Ca^{2+}]^{n_i}}{K^{n_i} + [Ca^{2+}]^{n_i}} \quad (1)$$

is the fraction of the fluorescence attributed to calcium binding to the high- or low-affinity sites, n_i is the Hill coefficient, and $[Ca^{2+}]$ is the free calcium ion concentration. For F154W, where calcium binding to the high-affinity sites accounts for the change in fluorescence intensity, f_2 was set to zero. Fits of the calcium titration data for F78W were obtained in two parts. For the first, covering the range pCa 9.5−6, $f_2 = 0$, and for the second, pCa 6−3.8, $f_1 = 0$. The fits were obtained using an iterative nonlinear least-squares procedure within the program MATLAB (Mathworks Inc.).

Fluorescence quenching data were obtained by adding acrylamide or iodide in approximately 0.01 M steps to yield a final concentration of 0.18 M. The quenching data were fitted to the Stern−Volmer equation

$$\frac{F_0}{F} = 1 + k_q \tau_0 [Q] \quad (2)$$

in which F_0 and F represent the integrated emission spectrum intensity in the absence and presence of acrylamide or iodide, k_q is the bimolecular rate constant, τ_0 is the lifetime of the fluorophore in the absence of quencher, and $[Q]$ is the concentration of quencher.

Absorption Spectroscopy. UV absorption spectra were measured at 20 °C using a CARY 2200 (Varian) spectrophotometer with an absorption bandwidth of 1 nm and cells with a path length of 0.5 or 1.0 cm. Aliquots of the protein stock were added to 8 M guanidine−HCl (GuHCl) to yield a final molar GuHCl concentration of 6 M. The concentration was then determined assuming a molar absorptivity for Trp at 280 nm of 5690 M^{-1} cm^{-1} (*42*). For wild-type TnC which lacks Trp residues, Phe was used for concentration determination and the molar absorptivity taken as 195 M^{-1} cm^{-1}/Phe residue. The spectra were corrected for turbidity by plotting the dependence of the log of the absorbance of the solution versus the log of the wavelength and extrapolating the linear dependence between these quantities in the range 320−400 nm to the absorption range 240−290 nm (*43*). The extrapolated value at the wavelength of maximum absorbance was then subtracted from the measured value. This procedure gave more consistent and reproducible results than amino acid analysis.

Circular Dichroism. Circular dichroism spectra were recorded using a J-710 spectropolarimeter (JASCO) equipped with a programmable temperature water bath (CTC-345, JASCO). For near-UV CD measurements (245−320 nm), rectangular cells with a path length of 1 cm and volume 1.5 mL were used while those in the far-UV CD (197−250 nm) employed U-type cells of path length 0.0148 cm and volume 0.045 mL. Wavelengths below 197 nm in the far-UV CD spectra were unattainable because of the high buffer absorbance. Protein concentrations were ≈50 μM for near- and far-UV CD measurements. Calcium titrations were conducted at 20 °C in the near- and far-UV using protein samples of concentration 55 and 11 μM, respectively. For these measurements, a volume of 2 mL and a cell of path length 0.5 cm were used. The far-UV CD titration data were analyzed using eq 1, where *f* is the normalized change in the CD signal, f_1 and f_2 are the fractions of the total far-UV CD change attributed to the high- and low-affinity sites, n_1 and n_2 are Hill coefficients, and K_1 and K_2 are the apparent affinity constants for calcium binding to the C- and N-terminal domain sites, respectively. CD spectra were recorded using a scan speed of 20 nm/min, a response time of 2 s, and a bandwidth of 2 nm for those in the far-UV and 1 nm for near-UV measurements. Typically, five spectra were accumulated and subsequently averaged. Temperature-dependent measurements were performed in the range 0−94 °C. The continuous temperature scan at fixed wavelength (222 nm) in the far-UV range was done using a scan rate of 50 °C/h and a response time of 8 s. Solvent evaporation was prevented by placing a drop of oil (that had been repeatedly boiled in water to remove soluble impurities) on top of the sample in the cell. The position of the temperature sensor of the CTC-345 unit was adjusted so that the temperature gradient between the cell holder and the solution in the cell at a scan rate of 50 °C/h was partially compensated for by the temperature gradient between the sensor and cell holder. Data are presented as molar ellipticity per residue using

$$[\theta]^{\lambda}_{MRW} = \frac{\theta^{\lambda}}{l C_{MRW}} \quad (3)$$

where θ^{λ} is the ellipticity in mdeg recorded by the instrument at wavelength λ, l is the path length in mm, and C_{MRW} is the molar concentration per residue, that is, the product of the molar protein concentration and the number of residues.

RESULTS

UV Absorbance. The UV absorption spectra of wt-TnC, F78W, and F154W are shown in Figure 1. The spectrum of wt chicken skeletal TnC, which lacks Trp and Tyr residues, shows the collective vibronic bands of the Phe residues at 252, 258, 264, and 269 nm. The absorption spectra of the mutants are characterized by the distinct band shapes of the Trp residue. An unusual feature of the absorption spectra of both mutants, and of F78W in particular, is the prominent ^1L_b vibronic band (*44*, *45*) at 291 nm (F78W) and 290 nm (F154W). The addition of calcium or magnesium results in a 1 nm red shift and an increase in the amplitude of the ^1L_b band of Trp-154 (data not shown) and is similar to that seen with Trp-152 of eel TnC (*46*). The ^1L_b band of Trp-78 is, however, unaffected by metal ion binding. The intensity of ^1L_a band of Trp-78 decreases in going from the apo to the calcium-saturated state while that of Trp-154 increases. The absorption spectra of F154W is similar to that of eel TnC

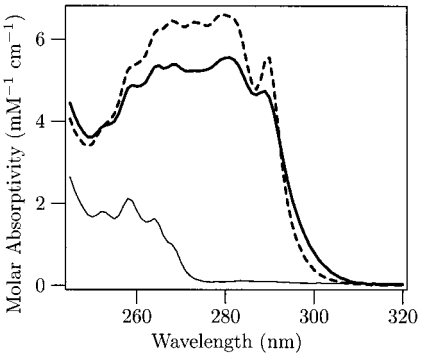

FIGURE 1: Turbidity-corrected absorption spectra of wt-TnC (—), F78W (- - -), and F154W (—) in the apo state. The sharp band at ≈290 nm in the spectra of the mutant proteins is the ^1L_b band of Trp. Protein concentration was ≈80 μM.

Table 1: Ratio of the Native Protein Molar Absorptivity at the Wavelength of Maximum Absorbance and That in 6 M GdHCl[a]

	$\epsilon^{\lambda_{max}}_{protein}/\epsilon^{\lambda_{max}}_{6MGdHCl}$
wt-TnC (λ_{max}, 258 nm)	1.090(4)
F78W (λ_{max}, 279 nm)	1.16(4)
F154W (λ_{max}, 280 nm)	0.975(5)

[a] Numbers in parentheses are the errors in the least significant digit.

(*46*), whose naturally occurring Trp residue (Trp-152) is in an equivalent position to Trp-154.

Table 1 gives the ratio of the extinction coefficient at the wavelength of maximum absorbance and that in 6 M GdHCl. These ratios allow a qualitative assessment of the similarity of the environments experienced by the Trp residue in the native and denatured states of the protein. For F154W, $\epsilon^{\lambda_{max}}_{protein}/\epsilon^{\lambda_{max}}_{6\ M\ GdHCl}$ is approximately 1 and is 16% higher for F78W. Thus, the environment experienced by Trp-154 in the native state is, within experimental error, identical to that in the denatured state, implying that Trp-154 is highly exposed to solvent. Trp-78, on the other hand, experiences a substantially different environment in the transition from the native to the denatured state with the implication being that it is buried in the native state.

Emission Spectra and Calcium Titrations. The Trp emission spectra of F154W and F78W in the apo and calcium-saturated (pCa 4) states are shown in Figure 2. In the apo state, the emission maximum (λ_{max}) of F154W is at 342 nm, which is almost identical to the value of 343 nm reported by Chandra et al. (*36*) for this mutant. Given that the corresponding value reported for Trp-152 of eel TnC is 352 nm (*46*), it would appear that the environment of the Trp residue in F154W is different from that of Trp-152 of eel TnC. However, this discrepancy appears to reside in the instruments used in the work of François et al. (*46*) and ours as the emission of apo-F154W, determined using a Perkin-Elmer MPF-66 spectrofluorometer, was 350 nm. The binding of calcium or magnesium to F154W results in blue shifts of the λ_{max} value relative to that in the apo-protein. Thus, in the calcium- and magnesium-saturated states, the λ_{max} value was 320 nm corresponding to a blue shift of 22 nm relative to the apo state. Because of the relatively high concentration of magnesium required to saturate F154W, 40 mM as first noted by Chandra et al. (*36*) and confirmed in this work, we have used sedimentation equilibrium measurements to verify

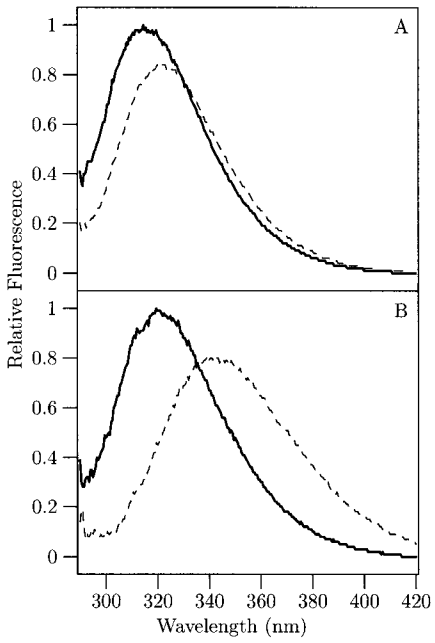

FIGURE 2: Fluorescence emission spectra of F78W (A) and F154W (B) in the apo (- - -) and calcium-saturated (—) (pCa 4.0) states. The excitation wavelength was 280 nm and the emission collected over the range 290−420 nm. The wavelength of maximum emission of Trp-154 is blue-shifted in the presence of metal ion relative to that of the apo state, while that of Trp-78 shows a small red shift in the calcium-saturated state relative to apo-F78W. Protein concentration was 7 μM.

that the F154W is monomeric under these conditions (data not shown). The λ_{max} of apo-F78W is at 313 nm. In the magnesium-saturated state, the λ_{max} value is also 313 nm, but the intensity of the emitted fluorescence is decreased. For the calcium-saturated state, the fluorescence intensity decreases further and the λ_{max} is at 323 nm, a red shift of 10 nm relative to the apo and magnesium-saturated states.

Figure 3 shows typical calcium titration curves obtained for the fluorescence change of F78W and F154W, while Table 2 summarizes the results obtained from an analysis of these and the far-UV CD titration data. The calcium titration curve for F154W is sigmoidal and represents titration of the high-affinity sites in the C-terminal domain. The recovered affinity constant for F154W ($-\log K_1$) of 6.73 is slightly higher than the value of 6.35 previously reported for this mutant (*36*). The calcium titration curve of F78W is more complex and consists of two apparently sigmoidal components. In the range of free calcium concentrations between pCa 9.5 and 6.0, the profile of the titration curve of F78W almost parallels that of F154W. However, at higher free calcium concentrations another transition is evident. Given the low protein concentrations used, it is unlikely that metal-ion-induced dimerization of these proteins occurs (*47*). Additionally, from an analysis of the time-dependent decay of the fluorescence anisotropy, we were unable to find evidence of dimerization (manuscript in preparation). By separately analyzing these regions, we obtained two apparent association constants. The first, $-\log K_1 = 6.91$, is consistent with binding to the high-affinity calcium/magnesium sites in the C-terminal domain while the second, $-\log K_2 = 5.55$ (see Table 2), likely reflects binding to the low-affinity sites in the N-terminal domain. When the calcium titration of F78W is performed in the presence of 5 mM magnesium

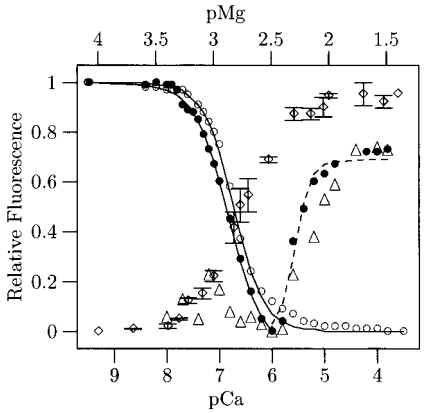

FIGURE 3: Calcium titration curves for F78W (●), F78W in the presence of 5 mM magnesium (△), and F154W (○) and the magnesium titration of F154W (◇). The two transitions in the titration curve of F78W (pCa 9.5−6 and pCa 6−3.5) are taken to reflect binding to the high- and low-affinity sites, respectively. The first transition (pCa 9.5−6) in the calcium titration of F78W is practically abolished in the presence of 5 mM magnesium while that of the second (pCa 6−3.8) remains. The solid lines (—) are fits to the data using eq 1 for F154W and the first transition of F78W, while the dashed (- - -) line is the fit to the second transition in the curve for F78W. The error bars for the magnesium titration data are the standard deviations obtained from three measurements. The errors for the calcium titrations are approximately 5%. Protein concentrations were 7−10 μM.

Table 2: Hill Coefficients and $-\log K_i$ Values for Wild-Type TnC (wt) and the Mutants F78W and F154W Obtained from Fluorescence and Far-UV CD Titrations[a]

	n_1	$-\log K_1$	n_2	$-\log K_2$
F78W[b]	1.5	6.91	2.5	5.55
F154W[b]	1.5	6.73		
wt-TnC[c]	1.5	7.09	1.6	5.69
F78W[c]	1.6	6.97	1.5	5.68
F154W[c]	2.0	6.87	2.0	5.66

[a] Fluorescence and CD titration data were analyzed using eq 1. The titration curve for F78W was fitted in two parts. The first covering the range pCa 9.5−6.0 was taken to reflect binding to the high-affinity sites while that from pCa 6−3.5 reflected binding to the low-affinity sites. The value of the Hill coefficient n_2 recovered from the biphasic fluorescence titration curve of F78W is greater than the theoretical maximum of 2.0 and reflects the nonindependence of the parameters of the fit for this dataset. [b] Data from fluorescence titrations. [c] Data from far-UV CD titrations.

(see Figure 3), the first transition—which reflects binding to the high-affinity sites—is substantially diminished while the second is virtually unaffected. This suggests that Trp-78 detects calcium binding at the C- as well as the N-terminal domain sites.

Acrylamide and Iodide Quenching. The quenching of the emitted fluorescence by acrylamide or iodide is widely used to probe the solvent accessibility of fluorescing groups in proteins (*48*). Stern−Volmer plots for the quenching of the fluorescence from Trp-78 and Trp-154 by acrylamide are presented in Figure 4. With both quenchers, fits to the Stern−Volmer equation (eq 2) for F78W and F154W were linear (correlation coefficient $\approx$ 0.99) and devoid of upward curvature which would be indicative of the presence of a static quenching component (*49*). The Stern−Volmer and bimolecular quenching constants for both acrylamide and iodide are given in Table 3.

Values for the bimolecular quenching constants (k_q) for the quenching of Trp fluorescence in proteins by acrylamide

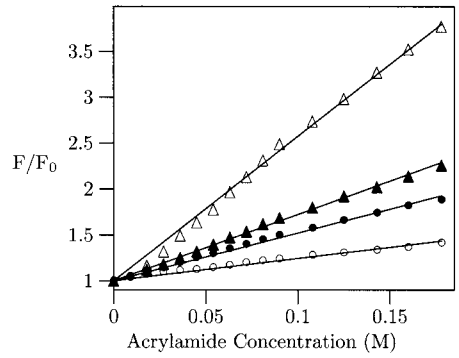

FIGURE 4: Stern−Volmer plots showing the quenching of the Trp fluorescence of the TnC mutants by acrylamide: apo-F78W (○); calcium-saturated (pCa 3.8) F78W (●); apo-F154W (△); calcium-saturated (pCa 3.8) F154W (▲). The solid lines are fits of the experimental data to the Stern−Volmer equation (eq 2). Protein concentration was 10 μM.

Table 3: Recovered Stern−Volmer and Bimolecular Quenching Constants for the Quenching of the Trp Fluorescence of F154W and F78W by Acrylamide and Iodide in the Apo and Calcium-Saturated States[a]

	acrylamide		iodide	
	K_{SV} (M^{-1})	k_q (M^{-1} s^{-1})	K_{SV} (M^{-1})	k_q (M^{-1} s^{-1})
F78W(apo)	2.2	5.7×10^8	0.8	2.1×10^8
F78W(Ca)	5.1	1.2×10^9	0.9	2.2×10^8
F154W(apo)	16.3	4.1×10^9	4.5	1.1×10^9
F154W(Ca)	7.2	2.2×10^9	2.0	5.9×10^8

[a] K_{SV} is given by the slope of the Stern−Volmer plot and is thus equal to $k_q\tau_0$. τ_0 values were obtained using time-correlated single photon counting (data not shown). The root mean square deviations for the k_q values were in the range 0.06−0.01.

range from 4×10^9 M^{-1} s^{-1} for a fully exposed residue to less than 0.5×10^9 M^{-1} s^{-1} for one buried in the protein matrix (*50*). The bimolecular quenching constant for free Trp by iodide is approximately 3×10^9 M^{-1} s^{-1} (*51*). Given the above, the calculated k_q value for the quenching of Trp-154 fluorescence by acrylamide suggests that this residue is fully exposed to solvent in the apo state. With iodide as quencher, the k_q value for apo-Trp-154 is lower than that of free Trp, suggesting that there are negative charges close to the indole side chain. Calcium binding to F154W results in a 2-fold reduction of the k_q values reported by both acrylamide and iodide, suggesting that the indole side chain of Trp-154 is "tucked" into the protein matrix under these conditions. For the quenching of the fluorescence from Trp-78 by acrylamide, the pattern observed for Trp-154 is reversed. Thus, the k_q value in the calcium-saturated state for F78W is greater, by a factor of 2, than that observed in the apo state. Interestingly, the k_q values for the quenching of the fluorescence from Trp-78 by iodide in the apo and calcium-saturated states are almost identical. However, the 5-fold difference in k_q values for the quenching by acrylamide and iodide suggests that there are negative charges close to Trp-78 in the calcium-saturated state. On the basis of the acrylamide data, Trp-78 is less buried in the calcium-bound state than in the apo state.

Far-UV CD. Figure 5 shows far-UV spectra of the TnC mutants in the apo and metal-bound states. The spectra—in both the apo and metal-bound states—are characterized by double minima at 208 and 222 nm, respectively, which are indicative of an α-helical structure. There are small differ-

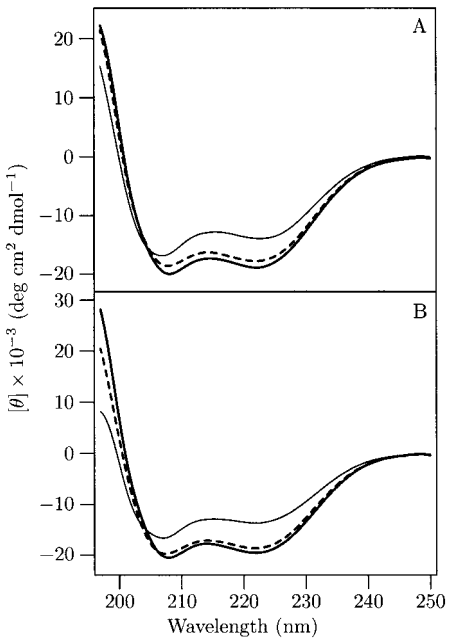

FIGURE 5: Far-UV CD spectra of F78W (A) and F154W (B) in the apo (—) and 3 mM magnesium- (- - -) and calcium-saturated (pCa 3.8) (—) states at 10 °C. Protein concentration was ≈55 μM.

Table 4: Molar Ellipticities at 222 nm and 10 °C for F78W and F154W

	$[\theta]_{222nm}$ (deg cm^2 dmol^{-1})		$[\theta]_{222nm}$ (deg cm^2 dmol^{-1})
F78W(apo)	−13 100	F154W(apo)	−13 700
F78W(Mg)	−17 800	F154W(Mg)	−18 700
F78W(Ca)	−18 900	F154W(Ca)	−19 600

ences in the molar ellipticity values of the apo and metal-bound states of both mutants. Table 4 gives the molar ellipticities at 222 nm for F78W and F154W in the apo and magnesium- and calcium-saturated states. At 222 nm, the difference between the magnesium- and calcium-saturated states of each mutant is approximately 5−6%. These values are comparable to those previously reported for F154W (*36*), rabbit skeletal muscle TnC (*9*), and wt chicken TnC (*40*). Titration by calcium or magnesium indicates that metal binding to the high-affinity sites and the resulting conformational events account for approximately 80% of the secondary structural changes in wt-TnC and the mutant proteins (data not shown).

Near-UV CD. The near-UV CD spectra of wt-TnC and the mutants F78W and F154W in the presence and absence of bound metal ions are shown in Figure 6. As with the near-UV absorbance spectra, the near-UV CD spectra of the wt protein are dominated by the signal from the Phe residues which occur at 255, 262, and 269 nm, respectively. Metal ion binding to either the high- or low-affinity sites does not result in an appreciable increase in the amplitude of the Phe bands. The small differences in the amplitude of the Phe bands in the wt protein result from differences in background of these bands caused by changes in the far-UV region. The near-UV CD spectra of F78W reveal that the strong Phe bands seen in the wt protein are substantially diminished with their amplitude being approximately one-third that of the wt protein. The ^1L_a and ^1L_b absorption bands of Trp are clearly resolved in the apo and magnesium- and calcium-saturated

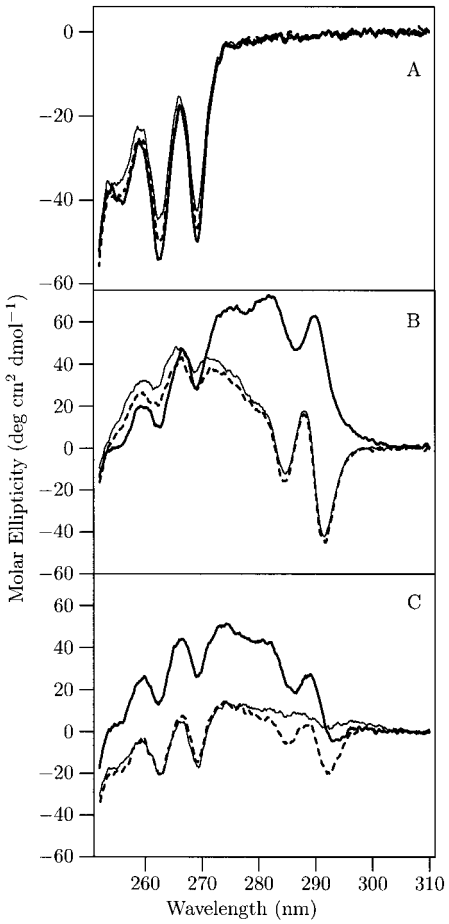

FIGURE 6: Near-UV CD spectra of wt-TnC (A), F78W (B), and F154W (C) in the apo (—) and 3 mM magnesium- (- - -) and calcium-saturated (pCa 3.8) (—) states at 10 °C. Note that the scale of the spectra for wt-TnC is expanded by a factor of 2 relative to those of the TnC mutants. Protein concentration was 55 μM.

states. The ^1L_b CD profiles in the apo and magnesium states are very similar as expected since magnesium binding occurs in the C-terminal domain and are characterized by two sharp negative bands at 285 and 292 nm. In the calcium-saturated state, however, the ^1L_b bands become positive and are clearly observed at 275, 282, and 290 nm. For this mutant, the intensity of the ^1L_a absorption is practically the same in the apo and magnesium- and calcium-saturated states.

The near-UV CD spectrum of F154W in the apo state is characterized by strong Phe bands having amplitudes equivalent to two-thirds those of the wt protein. For this mutant, the intensity of the ^1L_b bands in the apo state is significantly diminished relative to that of F78W. Despite the lack of intensity, two ^1L_b peaks can be discerned at 285 and 292 nm. Magnesium binding results in an increase in the amplitude of the 285 and 292 nm ^1L_b bands while those of Phe and the ^1L_a band of Trp are unchanged. The dissimilarity of the near-UV CD spectra of the magnesium- and calcium-saturated states of F154W suggests that the environments experienced by the Trp residue in these states are different.

The addition of calcium to F154W results in changes to both the ^1L_a and ^1L_b absorption bands of Trp while titration by magnesium effects changes in the ^1L_b band only (Figure 6). For F78W, titration by magnesium resulted in practically no change in the near-UV CD signal. However, the ^1L_b absorption band of Trp-78 is sensitive to the titration of sites

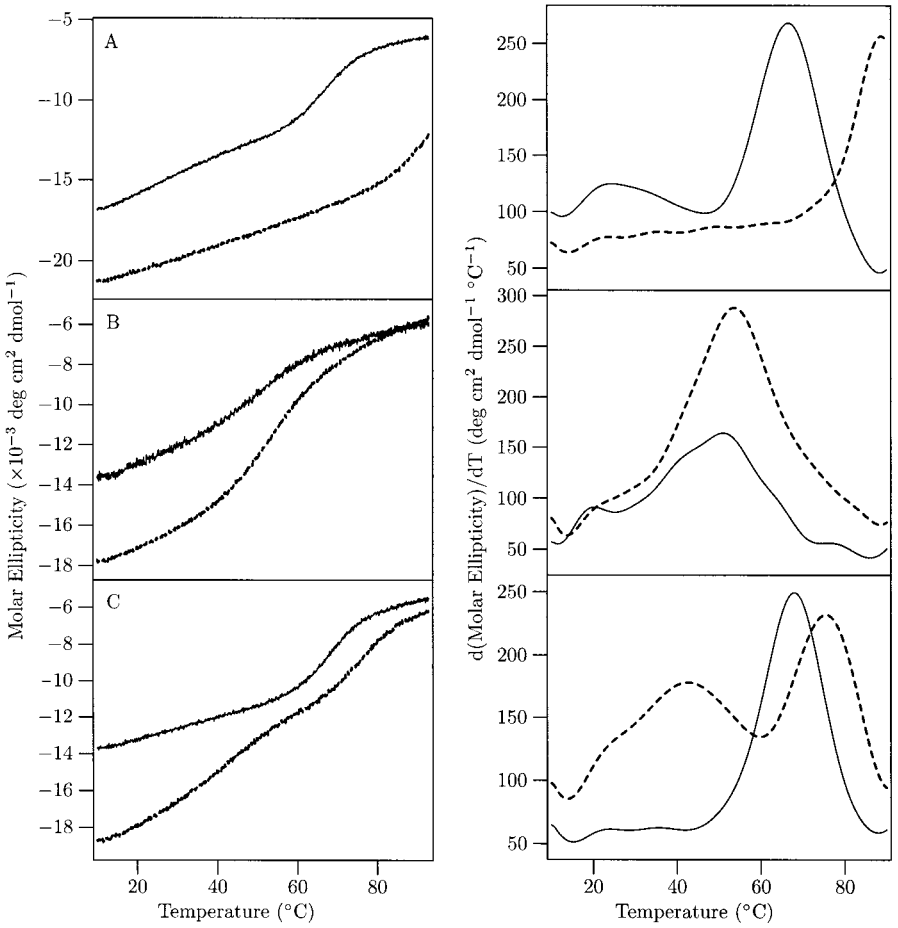

FIGURE 7: Temperature dependence of the CD signal at 222 nm (left panel) of wt-TnC (A), F78W (B), and F154W (C) in the apo (—) and magnesium-bound states (- - -). The panel on the right shows the first derivative curves after smoothing the corresponding data curves in the left panel. Protein concentrations were ≈55 μM.

III and IV in the COOH-terminal domain of the protein (data not shown).

Temperature Stability. In order to assess the effect of the Phe → Trp substitution on the stability of TnC mutants, the temperature-dependent profiles of these proteins and wt-TnC were measured in the far- and near-UV CD. The temperature curves obtained in the far-UV for the apo and magnesium-saturated states of wt-TnC, F78W, and F154W are shown in Figure 7. The midpoints of the transition(s) consistent with the temperature profiles were obtained by smoothing the temperature profile data using a Fourier transform algorithm (*52*) and taking the first derivative of the resulting data. The temperature transitions obtained from an analysis of the melting profiles measured in the near-UV and far-UV CD are summarized in Figure 8. For F154W, the derivative of the far-UV CD temperature curve for the apo state yields a single peak at 68 °C with a $\Delta_{1/2}$ of 20 °C. Magnesium binding to sites III and IV results in the appearance of two peaks in the derivative curve. The first is broad ($\Delta_{1/2}$ = 35 °C) and occurs at 42 °C while the second at 75 °C has $\Delta_{1/2}$ of 19 °C. The near-UV CD melting profile of F154W, which reflects melting of the C-terminal domain, consists of a single peak at 42 °C in the magnesium-saturated state. Therefore, the temperature transition at 75 °C observed in the far-UV CD melting profile of the magnesium-bound state can be assigned to the melting of the N-terminal domain. It has been shown that in the apo state the secondary structure content of the N-terminal domain is greater than that of the C-terminal

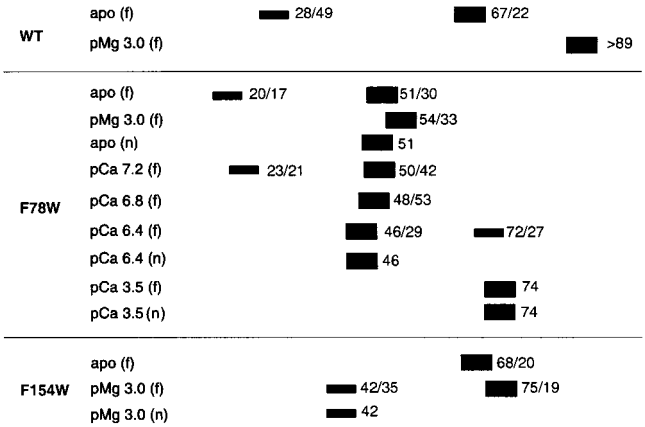

FIGURE 8: Summary of the near-UV CD (n) and far-UV CD (f) melting of wt-TnC, F78W, and F154W. The filled rectangles represent the positions of the derivative of the temperature curves for the protein samples in the presence and absence of bound metal ions. Thick and thin rectangles represent the melting of the NH_2- and COOH-terminal domains, respectively. Numbers to the right of the rectangles are the peak positions and approximate $\Delta_{1/2}$ in °C.

domain (*29*, *53*). Consequently, the C-terminal domain in the apo state is expected to melt before the N-terminal. On this basis, the 68 °C transition of apo-F154W can be assigned to the melting of the N-terminal domain.

Given the preceding, the temperature transition occurring at 67 °C in wt-TnC is due to the melting of the N-terminal

domain while that at 28 °C is due to the C-terminal domain. The single transition in the presence of magnesium is assigned to the NH_2-terminal domain, and the transition corresponding to the melting of the COOH-terminal domain presumably occurs at greater than 90 °C. These assignments are in good agreement with those of Brzeska et al. (*29*), who studied the thermal stability of the isolated NH_2- and COOH-terminal fragments of rabbit skeletal TnC under various conditions. In their work, the NH_2-terminal fragment (residues 9−84) melts at 60 °C in the apo state and 68 °C in the presence of magnesium, while the COOH-terminal fragment (residues 89−159) melts at 20 °C in the apo state and 83 °C when magnesium is bound. For F78W, the transition at 51 °C in the far-UV CD melting curve of the apo state is assigned to the melting of the NH_2-terminal domain as the temperature transition in the corresponding near-UV CD melting curve is at the same temperature. The transition at 20 °C corresponds to the melting of the COOH-terminal domain of F78W. The effect of increasing the calcium ion concentration on the transition temperature of F78W is shown in Figure 8. At pCa 7.2, the COOH-terminal domain which melts at 20 °C in the apo state shifts to 23 °C while the transition corresponding to the NH_2-terminal domain was at 50 °C. Increasing the calcium ion concentration to pCa 6.8 results in a single broad transition at 48 °C while at pCa 6.4 two transitions are again observed. The one at 46 °C from measurements in the near-UV CD corresponds to the melting of the NH_2-terminal domain. The other at 72 °C is the transition for the melting of the COOH-terminal domain now stabilized by the binding of calcium. The melting data indicate that the stabilities of the domains of TnC are not influenced only by direct metal ion binding to their respective sites. Consequently, metal ion binding to sites III and IV influences the stability of the N-terminal domain.

DISCUSSION

The principal objectives of this work are interpretation of the optical spectroscopic properties of the TnC mutants in terms of a physical model of the conformational changes these proteins undergo when they bind metal ions and to enable inferences regarding interdomain interaction. To achieve the first requires that we understand how the optical properties of Trp or of the protein main chain (far-UV CD) translate physicochemically.

The fluorescence of Trp in proteins depends on the environment of the indole ring, and the wavelengths of maximum emission (λ_{max}), corrected for the wavelength dependence of the monochromator response, range from 308 nm for Trp-48 of azurin (*54*−*56*) which is buried in a hydrophobic pocket to 352 nm (*57*), the latter being similar to that of zwitterionic Trp in water at pH 7.0. For Trp residues which have emission λ_{max} values between these extremes, the environment of the Trp residue is usually expressed in relative terms. Given the utility of Trp fluorescence in the study of macromolecules, there have been several studies aimed at elucidating the factors that influence the fluorescence emitted from Trp in proteins. Recently, on the basis of quantum chemical calculations and molecular dynamics simulations, Callis et al. (*58*) have made remarkable progress in making accurate predictions regarding the position of the Trp fluorescence emission maximum in proteins. On the basis of their studies, they concluded that the λ_{max} values for Trp in proteins is predominantly determined by the local electric field projection along the long-axis of the indole ring. For Trp-containing proteins whose λ_{max} values are between the two extremes stated above, the model of Callis et al. predicts a blue shift ($\approx \geq 10$ nm) in the λ_{max} value on cooling if water relaxation contributes significantly to the observed red shift. We have measured the emission spectra of the TnC mutants in a 66.7% glycerol−water solution at −45 °C (data not shown) and have found that the λ_{max} values for the apo and calcium-saturated states of F154W are shifted by 22 and 14 nm, respectively. The corresponding shift for both the apo and calcium-saturated states of F78W was 10 nm. Thus, if Callis' model is correct, it appears that water relaxation, especially in the case of apo-Trp-154, is predominantly responsible for the λ_{max} obtained.

The results from the spectrophotometric data, fluorescence quenching, and the Trp fluorescence emission maximum suggest that, in the apo state, Trp-78 is not exposed to solvent. These data are consistent with the 0 Å^2 solvent accessible surface area calculated for Phe-78 using the program NAOMI (*59*) applied to the X-ray crystal structure of chicken skeletal TnC (*2*) in which only the C-terminal domain sites had calcium ions. The red shift in the position of the λ_{max} value and the increased k_q value on calcium binding suggest an increase in the solvent accessibility of this residue. This is also consistent with crystallographic data for the homologous residue, Phe-75 of rabbit skeletal TnC, in the calcium-saturated state (*21*) for which the solvent accessible surface area is 3 Å^2. Given the bulky indole side chain, it is likely that the accessible surface area for Trp-78 is somewhat larger than that of Phe-75. For F154W, the quenching and absorption data as well as the position of the emission λ_{max} value suggest that the indole moiety is substantially exposed to solvent in the apo state. On binding metal ions, the λ_{max} value is blue-shifted relative to its value in the apo state. The fact that calcium and magnesium ion binding to the high-affinity sites induce similar blue shifts suggests that the environments of Trp-154 in these two states of the protein are similar. There have been several reports suggesting that while the overall fold of the C-terminal domain in both the calcium- and magnesium-bound states are similar, differences exist in proton resonances corresponding to residues of the aromatic cluster (*60*, *61*). In the X-ray crystal structure of pike parvalbumin (pI = 4.10), which has magnesium bound to the EF-site (*62*), only one carboxylate oxygen of Glu-101, which is homologous to Glu-153 in chicken skeletal TnC, is coordinated to the metal ion. The other carboxylate oxygen of Glu-101 is hydrogen-bonded to an additional water molecule. In the calcium-bound state, both oxygens of Glu-101 are coordinated to the metal ion and there is one water molecule in the EF-site. If magnesium binding to TnC is analogous to that in parvalbumin, the additional water molecule could in principle change the character of the environment of the Trp residue sufficiently to make the emission from the calcium- and magnesium-saturated states different. The identical emission λ_{max} value of Trp-154 in the calcium- and magnesium-bound states suggests that the putative additional water molecule in the magnesium-bound state does not influence the fluorescence from Trp-154 as presumably occurs in eel TnC (*46*).

The calcium titration data for F154W indicates that the fluorescence emission from Trp-154 is sensitive to ligand binding at the high-affinity sites. Chandra et al. (*36*) report a 2-fold reduction in the calcium binding affinity of the C-terminal domain sites of F154W relative to the wild-type protein, and this finding is consistent with our results. The recovered apparent association constant for calcium binding to the high-affinity sites of F154W is also lower than that of eel TnC (*63*), which has a naturally occurring Trp residue in a position analogous to that of Trp-154 in chicken TnC. For the low-affinity sites of F154W, the apparent association constants are similar to those obtained for the wild-type protein, suggesting that the calcium affinity of these sites was not affected by the mutation in the C-terminal domain. Additionally, as is evident from the affinity constants recovered from the far-UV CD titration (see Table 2), the replacement of Phe-78 by Trp did not significantly affect the calcium affinity of either the low- or high-affinity sites of F78W. The latter finding is consistent with simulations we have conducted (data not shown) using minimum perturbation mapping (*64*) which suggested that the Phe → Trp replacements could be accommodated without adversely disrupting the structure of TnC.

Given the similarity of the metal-binding properties of the TnC mutants—especially those of F78W—to wt-TnC, and their ability to regulate muscle contraction, it is tempting to conclude that the Phe → Trp replacement is effectively "neutral". The first hint suggesting that this is perhaps not so is seen in Table 4. Although the absolute value of the difference ($[\theta]_{222nm}^{F78W} - [\theta]_{222nm}^{F154W}$) for the apo states of the mutants is close to the experimental error in these measurements, the lower molar ellipticity value of F78W suggests that the introduction of Trp-78 in the N-terminal domain causes a greater reduction in the secondary structure content in comparison to Trp-154. This is consistent with the notion that, in the apo state, the C-terminal domain of TnC is relatively disordered while the N-terminal domain is ordered (*65*, *66*) as has been demonstrated in calmodulin (*67*, *68*). Additional information regarding the effect of the introduced Trp residues is found in the temperature-dependent CD measurements. On the basis of our assignments and contrary to our expectations and those of Chandra et al. (*36*), the introduction of Trp-154 destabilizes the C-terminal domain of F154W—with minimal effect on the stability of the N-terminal domain—in the apo state with respect to temperature, even though functional integrity is maintained. This suggests that, in wt-TnC, Phe-154 may be a part of an element of secondary structure or, alternatively, it interacts with elements of secondary and/or tertiary structure which become disrupted by the substitution with a more bulky Trp residue. In like manner, the introduction of Trp-78 in the N-terminal domain destabilizes that domain.

An important finding of the present study regards the evidence supporting interactions between the N- and C-terminal domains of TnC. The titration data of F78W show that the fluorescence of Trp-78 is sensitive to calcium binding at the C-terminal domain sites. This result was confirmed by calcium titrations of F78W monitored using near-UV CD (data not shown) as well as calcium titrations in the presence of 5 mM magnesium (see Figure 3). Additionally, from the thermal stability measurements it is apparent that "events" occurring in the N-terminal domain influence the stability of the C-terminal domain and vice versa. Thus, (a) magnesium binding to the C-terminal domain of wt-TnC increases the stability of the N-terminal domain, (b) the Phe → Trp mutation has a destabilizing effect not only on the N-terminal domain of F78W but also on the C-terminal domain, (c) the binding of calcium to the C-terminal domain sites of F78W increases the stability of this domain but decreases that of the N-terminal domain, and (d) magnesium binding to the high-affinity sites of F154W stabilizes the N-terminal domain. It is interesting to note that magnesium binding to the C-terminal domain sites stabilizes the N-terminal domain of both wt-TnC and the two mutant proteins. However, for F78W, calcium binding to these sites destabilizes the N-terminal domain. The effect of interdomain interaction on domain stability in TnC is somewhat akin to that recently observed in calmodulin where such interactions are apparently responsible for a 10 °C stabilization of the apo domain (*69*). The present observation of interaction between the domains of TnC is consistent with those of Grabarek et al. (*24*) and Ellis et al. (*26*). These groups found that calcium binding to the N-terminal domain sites induces conformational changes in the high-affinity sites and that the chemical shift of cadmium ions bound to sites I and II was sensitive to metal in sites III and IV, respectively. The mechanism by which the interdomain interaction just described occurs is not known. Additionally, the circumstances that facilitate its detection are not obvious. Johnson et al. (*70*), for example, found evidence of interdomain interaction when Met-25 in the N-terminal domain of TnC was labeled with dansylaziridine. However, a study using a F29W mutant of TnC (*41*) found no evidence of interactions between the domains of TnC. Given the large distance separating the metal-binding sites in the N- and C-terminal domains, approximately 40 Å from the crystal structures of TnC in which the high-affinity sites saturated by calcium ions (*2*) and that in which all sites are occupied by calcium (*21*) would likely preclude long-range electrostatic interactions. An explanation for the observed interdomain interaction involves the existence of conformations which allow the N- and C-terminal domains of TnC to be in close proximity. The energy transfer studies of Wang et al. (*71*) indicate that at neutral pH the distance between the calcium binding sites is substantially decreased relative to that seen in the crystal structure. Other studies (*72*) have suggested that the distances between the N- and C-terminal domains of TnC are not fixed but are a function of solution conditions and metal ion occupancy of the protein.

In summary, it has been shown that the mutation of Phe-78 to Trp in chicken skeletal TnC does not significantly affect metal ion binding to the high- or low-affinity sites in contrast to the Phe-154 to Trp mutation which reduces the calcium-binding affinity of sites III and IV. The spectral properties of Trp-154 suggest that this residue is highly exposed to solvent in the apo state. Metal ion binding to the C-terminal domain sites results in a reduction of the solvent accessibility of Trp-154 so that this residue is essentially buried. The solvent accessibility of Trp-78 increases on going from the apo to the calcium-saturated states. The calcium titration data for F78W and a study of the thermal stability of the mutant in the apo and metal-bound states strongly suggest that interactions between the N- and C-terminal of TnC occur. Since the optical spectroscopic properties of the introduced

Trp residues are sensitive to the conformational transitions occurring in TnC, they should prove useful in studying the dynamic behavior of the N- and C-terminal domains of this protein.

ACKNOWLEDGMENT

The authors thank the reviewers for their helpful comments and for suggesting the calcium titration of F78W in the presence of saturating concentrations of magnesium.

REFERENCES

1. Herzberg, O., and James, M. N. G. (1985) *Nature 313*, 653−659.
2. Satyshur, K. A., Rao, T. S., Pyzalska, D., Drendel, W., Greaser, M., and Sundaralingam, M. (1988) *J. Biol. Chem. 263*, 1628−1647.
3. Kretsinger, R. H., and Nockolds, C. E. (1973) *J. Biol. Chem. 248*, 3313−3326.
4. Potter, J. D., and Gergely, J. (1975) *J. Biol. Chem. 250*, 4628−4633.
5. Zot, A. S., and Potter, J. D. (1987) *Ann. Rev. Biophys. Biophys. Chem. 16*, 535−559.
6. Negele, J. C., Dotson, D. G., Liu, W., Sweeny, H. L., and Putkey, J. A. (1992) *J. Biol. Chem. 267*, 825−831.
7. Sorenson, M. M., Da Silva, A. C. R., Gouveira, C. S., Sousa, V. P., Oshima, W., Ferro, J. A., and Reinach, F. C. (1995) *J. Biol. Chem. 270*, 9770−9777.
8. Szczesna, D., Guzman, G., Miller, T., Zhao, J., Farokhi, K., Ellemberger, H., and Potter, J. D. (1996) *J. Biol. Chem. 271*, 8381−8386.
9. Johnson, J. D., and Potter, J. D. (1978) *J. Biol. Chem. 253*, 3775−3777.
10. Herzberg, O. H., Moult, J., and James, M. N. G. (1986) *J. Biol. Chem. 261*, 2638−2644.
11. Grabarek, Z., Tan, R.-Y., Wang, J., Tao, T., and Gergely, J. (1990) *Nature 345*, 132−135.
12. Fujimori, K., Sorenson, M., Herzberg, O., Moult, J., and Reinach, F. (1990) *Nature 345*, 182−184.
13. Lin, X., Krudy, G. A., Howarth, J., Brito, R. M., Rosevear, P. R., and Putkey, J. A. (1994) *Biochemistry 33*, 14434−14442.
14. Gagné, S. M., Tsuda, S., Li, M. X., Chandra, M., Smillie, L. B., and Sykes, B. D. (1994) *Protein Sci. 3*, 1961−1974.
15. Ingraham, R. H., and Hodges, R. S. (1988) *Biochemistry 27*, 5891−5898.
16. Fuchs, F., Liou, Y. M., and Grabarek, Z. (1989) *J. Biol. Chem. 264*, 20344−20349.
17. Putkey, J. A., Dotson, D. G., and Mouawad, P. (1993) *J. Biol. Chem. 268*, 6827−6830.
18. Ikura, M., Clore, G. M., Gronenborn, A. M., Zhu, G., Klee, C. B., and Bax, A. (1992) *Science 256*, 632−638.
19. Meador, W. E., Means, A. R., and Quiocho, F. A. (1992) *Science 257*, 1251−1255.
20. Slupsky, C. M., and Sykes, B. D. (1995) *Biochemistry 34*, 15953−15964.
21. Houdusse, A., Love, M. L., Dominguez, R., Grabarek, Z., and Cohen, C. (1997) *Structure 5*, 1695−1711.
22. Strynadka, N. C., Cherney, M., Sielecki, A. R., Li, M. X., Smillie, L. B., and James, M. N. G. (1997) *J. Mol. Biol. 273*, 238−255.
23. Levine, B. A., Mercola, D., Coffman, D., and Thornton, J. M. (1977) *J. Mol. Biol. 115*, 743−760.
24. Grabarek, Z., Leavis, P. C., and Gergely, J. (1986) *J. Biol. Chem. 261*, 608−613.
25. Seamon, K. B., Hartshorne, D. J., and Bothner-By, A. A. (1977) *Biochemistry 16*, 4039−4046.
26. Ellis, P. D., Marchetti, P. S., Strang, P., and Potter, J. D. (1988) *J. Biol. Chem. 263*, 10284−10288.
27. Pedigo, S., and Shea, M. A. (1995) *Biochemistry 34*, 1179−1196.
28. Shea, M. A., Verhoeven, A. S., and Pedigo, S. (1996) *Biochemistry 35*, 2943−2957.
29. Brzeska, H., Venyaminov, S., Grabarek, Z., and Drabikowski, W. (1983) *FEBS Lett. 153*, 169−173.
30. Leavis, P. C., Rosenfeld, S. S., Gergely, J., Grabarek, Z., and Drabikowski, W. (1978) *J. Biol. Chem. 253*, 5452−5459.
31. François, J.-M., Sheng, Z., Szczesna, D., and Potter, J. D. (1995) *J. Biol. Chem. 270*, 19287−19293.
32. She, M., Dong, W. J., Umeda, P. K., and Cheung, H. C. (1997) *Biophys. J. 73*, 1042−1055.
33. Akella, A. B., Su, H., Sonnenblick, E. H., Rao, V. G., and Gulati, J. (1997) *J. Mol. Cell. Cardiol. 29*, 381−389.
34. Gryczynski, I., Malak, H., Lakowicz, J. R., Cheung, H. C., Robinson, J., and Umeda, P. K. (1996) *Biophys. J. 71*, 3448−3453.
35. Foguel, D., Suarez, M. C., Barbosa, C., Rodrigues, J. J., Sorenson, M. M., Smillie, L. B., and Silva, J. L. (1996) *Proc. Natl. Acad. Sci. U.S.A. 93*, 10642−10646.
36. Chandra, M., McCubbin, W. D., Oikawa, K., Kay, C. M., and Smillie, L. B. (1994) *Biochemistry 33*, 2961−2969.
37. Tsalkova, T. N., and Privalov, P. L. (1985) *J. Mol. Biol. 181*, 533−544.
38. Miller, T. (1990) *Isolation and characterization of the rat liver connexin-32 gene*, Ph.D. Thesis, University of Miami.
39. Robertson, S. P., and Potter, J. D. (1984) in *Methods in Pharmacology* (Schwartz, A., Ed.) Vol. 5, pp 63−75, Plenum Press, New York.
40. Golosinska, K., Pearlstone, J. R., Borgford, T., Oikawa, K., Kay, C. M., Carpenter, M. R., and Smillie, L. B. (1991) *J. Biol. Chem. 266*, 15797−15809.
41. Pearlstone, J. R., Borgford, T., Chandra, M., Oikawa, K., Kay, C. M., Herzberg, O., Moult, J., Herklotz, A., Reinach, F. C., and Smillie, L. B. (1992) *Biochemistry 31*, 6545−6553.
42. Edelhoch, H. (1967) *Biochemistry 6*, 1948−1954.
43. Winder, A. F., and Gent, W. L. (1971) *Biopolymers 10*, 1243−1251.
44. Platt, J. R. (1949) *Chem. Phys. 17*, 484−495.
45. Valeur, B., and Weber, G. (1977) *Photochem. Photobiol. 25*, 441−444.
46. François, J.-M., Sedarous, S. S., and Gerday, C. (1997) *J. Muscle Res. Cell Motil. 18*, 323−334.
47. Margossian, S. S., and Stafford, W. S. (1982) *J. Biol. Chem. 257*, 1160−1165.
48. Eftink, M. (1991) in *Topics in fluorescence spectroscopy* (Lackowicz, J. R., Ed.) Vol. 2, Chapter 2, pp 53−120, Plenum Press, New York.
49. Lakowicz, J. R. (1983) *Principles of Fluorescence Spectroscopy*, Plenum Press, New York.
50. Eftink, M. R., and Ghiron, G. A. (1976) *Biochemistry 15*, 672−680.
51. Permyakov, E. A. (1993) *Luminescent spectroscopy of proteins*, CRC Press, Boca Raton, FL.
52. Press, W. H., Flannery, B. P., Teukolsky, S. A., and Vetterling, W. T. (1993) *Numerical recipes in C*, Cambridge University Press, Cambridge, U.K.
53. Fredricksen, R. S., and Swenson, C. A. (1996) *Biochemistry 35*, 14012−14026.
54. Hutnik, C. M., and Szabo, A. G. (1989) *Biochemistry 28*, 3923−3934.
55. Szabo, A. G., Stepanik, T. M., Wayner, D. M., and Young, N. M. (1983) *Biophys. J. 41*, 233−244.
56. Turoverov, K. K., Kuznetsova, I. M., and Zaitsev, V. N. (1985) *Biophys. Chem. 23*, 79−89.
57. Longworth, J. W. (1971) in *Excited states of proteins and nucleic acids* (Steiner, R., and Weinryb, I., Eds.) Chapter 6, pp 319−474, Plenum Press, New York.
58. Callis, P. R., and Burgess, B. K. (1997) *J. Phys. Chem. B 101*, 9429−9432.
59. Brocklehurst, S. M., and Perham, R. N. (1993) *Protein Sci. 2*, 626−639.
60. Levine, B. A., Thornton, J. M., Fernandes, R., Kelly, C. M., and Mercola, D. (1978) *Biochim. Biophys. Acta 535*, 11−24.

61. Drabikowski, W., Dalgarno, D. C., Levine, B. A., Gergely, J., Grabarek, Z., and Leavis, P. C. (1985) *Eur. J. Biochem. 151*, 17−28.
62. Declercq, J. P., Tinant, B., Parello, J., and Rambaud, J. (1991) *J. Mol. Biol. 220*, 1017−1039.
63. François, J.-M., Gerday, C., Prendergast, F. G., and Potter, J. D. (1993) *J. Muscle Res. Cell Motil. 14*, 585−593.
64. Haydock, C. (1993) *J. Chem. Phys. 98*, 8199−8214.
65. Leavis, P. C., and Gergely, J. (1984) *Crit. Rev. Biochem. 16*, 235−305.
66. Shaw, G. S., and Sykes, B. D. (1996) *Biochemistry 35*, 7429−7438.
67. Drabikowski, W., Brzeska, H., and Venyaminov, S. Y. (1982) *J. Biol. Chem. 257*, 11584−11590.
68. Tjandra, N., Kuboniwa, H., Ren, H., and Bax, A. (1995) *Eur. J. Biochem. 230*, 1014−1024.
69. Sorensen, B. R., and Shea, M. A. (1998) *Biochemistry 37*, 4244−4253.
70. Johnson, J. D., Collins, J. H., and Potter, J. D. (1978) *J. Biol. Chem. 25*, 6451−6458.
71. Wang, C.-L., Zhan, Q., Tao, T., and Gergely, J. (1987) *J. Biol. Chem. 262*, 9636−9640.
72. Cheung, H. C., Wang, C.-K., Gryczynski, I., Wiczk, W., Laczko, G., Johnson, M. L., and Lakowicz, J. R. (1991) *Biochemistry 30*, 5238−5247.

BI982048J